

ponse and its regulation are processes that require a complex interplay of a variety of agents, including cytokines. It is tempting to speculate that CICs generated during various types of immune responses may also participate in the immunoregulatory network by signalling through FcRs expressed on different classes of leukocytes.

1. Daeron, M., Fc receptor biology. *Annu. Rev. Immunol.*, 1997, **15**, 203–234.
2. Miescher, S. M. and Vogel, M., Molecular aspects of allergy. *Mol. Aspects Med.*, 2002, **23**, 413–462.
3. Henricks, P. A., Verhoef, J. and Nijkamp, F. P., Modulation of phagocytic cell function. *Vet. Res. Commun.*, 1986, **10**, 165–188.
4. Theofilopoulos, A. N. and Dixon, F.J., Immune complexes in human diseases: a review. *Am. J. Pathol.*, 1980, **100**, 531–594.
5. Procaccia, S. *et al.*, Rheumatoid factors and circulating immune complexes in HIV-infected individuals. *AIDS*, 1991, **5**, 1441–1446.
6. Raja, A., Uma Devi, K. R., Ramalingam, B. and Brennan, P. J., Immunoglobulin G, A, and M responses in serum and circulating immune complexes elicited by the 16-kilodalton antigen of *Mycobacterium tuberculosis*. *Clin. Diagn. Lab. Immunol.*, 2002, **9**, 308–312.
7. Trinchieri, G. and Valiante, N., Receptors for the Fc fragment of IgG on natural killer cells. *Nature Immunol.*, 1993, **12**, 218–234.
8. Buchwald, D. and Komaroff, A. L., Review of laboratory findings for patients with chronic fatigue syndrome. *Rev. Infect. Dis. Suppl. 1*, 1991, **13**, S12–S18.
9. Vulcano, M., Olabuenaga, S. E., Galassi, N., Felippo, M., Perez, Bianco, R. and de Bracco, M. M., Inhibition of normal natural killer cytotoxicity by sera from hemophilic patients. *Immunol. Lett.*, 1993, **36**, 153–159.
10. Guseva, S. A., Fedko, A. A. and Volobueva, Z. V., Suppressive effect of circulating immune complexes on cytotoxicity of blood lymphocytes in patients with chronic myeloid leukemia. *Gematol. Transfuziol.*, 1992, **37**, 10–12.
11. Struyf, N. J., Snoeck, H. W., Bridts, C. H., De Clerck, L. S. and Stevens, W. J., Natural killer cell activity in Sjogren's syndrome and systemic lupus erythematosus: stimulation with interferon and interleukin-2 and correlation with immune complexes. *Ann. Rheum. Dis.*, 1990, **49**, 690–693.
12. Bugis, S. P., Lotzova, E., Savage, H. E., Hester, J. P., Raczy, T., Sacks, P. G. and Schantz, S. P., Inhibition of lymphokine-activated killer cell generation by blocking factors in sera of patients with head and neck cancer. *Cancer Immunol. Immunother.*, 1990, **31**, 176–181.
13. Dhillon, S. and Saxena, R. K., Upregulation of KIR expression on murine bone marrow cells by paraformaldehyde fixed tumor cells. *Immunol. Lett.*, 1999, **70**, 157–163.
14. Udaykumar, Sarin, A. and Saxena, R. K., Analysis of circulating immune complexes (CIC) in tuberculosis: levels of specific antibody and antigens in CIC and relationship with serum antibody. *FEMS Microbiol. Immunol.*, 1991, **3**, 135–142.
15. Saxena, R. K., Saxena, Q. B. and Adler, W. H., Modulation of natural cytotoxicity by alloantibodies. V. The mechanism of a selective augmenting effect of anti-H-2 antisera on the natural killer activity of mouse spleen cells. *Cell Immunol.*, 1981, **65**, 115–130.
16. Saxena, R. K., Saxena, Q. B. and Adler, W. H., Properties and characterization of a rat spleen cell-derived factor that induces resistance to natural killer cell lysis in YAC lymphoma cells. *J. Immunol.*, 1988, **141**, 1782–1787.
17. Bayer, A. S., Theofilopoulos, A. N., Tillman, D. B., Dixon, F. J. and Guze, L. B., Use of circulating immune complex levels in the serodifferentiation of endocarditic and nonendocarditic septicemias. *Am. J. Med.*, 1979, **66**, 58–62.
18. Gamberale, R., Giordano, M., Trevani, A. S., Andonegui, G. and Geffner, J. R., Immune complexes inhibit apoptosis of chronic lymphocytic leukaemia B cells. *J. Immunol.*, 1998, **161**, 3666–3674.
19. Thien, M., Renger, D., Deicher, H. and Pichler, W. J., *Rheumatol. Int.*, 1985, **5**, 127–132.
20. Gamberale, R. *et al.*, *Br. J. Haematol.*, 1999, **107**, 870–876.
21. Ptak, W., Paliwal, V., Bryniarski, K., Ptak, M. and Askenase, P. W., Aggregated immunoglobulin protects immune T cells from suppression: dependence on isotype, Fc portion, and macrophage Fc gamma R. *Scand. J. Immunol.*, 1998, **47**, 136–145.
22. Schattner, M., Lazzari, M., Trevani, A. S., Malchiodi, E., Kempfer, A. C., Isturiz, M. A. and Geffner, J. R., Activation of human platelets by immune complexes prepared with cationized human IgG. *Blood*, 1993, **82**, 3045–3051.
23. Saxena, R. K., Wiessman, D., Saxena, Q. B., Simpson, J. and Lewis, D. M., Kinetics of changes in lymphocyte sub-populations in mouse lungs after intrapulmonary infection with *M. bovis* (Bacillus Calmette-Guerin) and identity of cells responsible for IFN gamma responses. *Clin. Exp. Immunol.*, 2002, **128**, 405–410.
24. Saxena, R. K., Valliyathan, V. and Lewis, D. M., Evidence for lipopolysaccharide-induced differentiation of RAW264.7 murine macrophage cell line into dendritic like cells. *J. Biosci.*, 2003, **28**, 129–134.

ACKNOWLEDGEMENT. This work was supported by a CSIR research grant to R.K.S. A.D. received a UGC fellowship.

Received 1 August 2003; revised accepted 7 May 2004

Differential response of winter cooling on biological production in the northeastern Arabian Sea and northwestern Bay of Bengal

R. Jyothibabu*, P. A. Maheswaran, N. V. Madhu, T. T. Mohammed Ashraf, Vijay John Gerson, P. C. Haridas, P. Venugopal, C. Revichandran, K. K. C. Nair and T. C. Gopalakrishnan

National Institute of Oceanography, Regional Centre, PB No. 1913, Kochi 682 018, India

The northern parts of the twin seas bordering the Indian subcontinent, the Arabian Sea (AS) and Bay of Bengal (BOB), were studied during the winter monsoon. Higher biological production was observed in the AS (chlorophyll *a* 47.5 mg m⁻², primary production 1114 mgC m⁻² d⁻¹, mesozooplankton biomass 175 mmolC m⁻², microzooplankton biomass 26 mmolC m⁻²) compared to the BOB (chlorophyll *a* 10.3 mg m⁻², primary production 117 mgC m⁻² d⁻¹, mesozooplankton biomass 71 mmolC m⁻², microzooplankton biomass 10.6 mmolC m⁻²). In the AS, winter cooling assisted by the high surface salinity (>36) resulted in densification of surface layers, con-

*For correspondence. (e-mail: rjyothi1@yahoo.co.in)

vective mixing and deepening of the mixed layer (average 60 m). Convective mixing brought nutrients to the upper euphotic column (~2 μM nitrate in the top 50 m) and stimulated biological production. The northern part of the BOB, however, responded differently to atmospheric cooling. The prevailing low salinity (27) resulted in thermal inversion and stratification of the water column. Shallow mixed layer (average < 15 m) and the absence of nitrate in the top 50 m water column were the reasons for low biological production. Our results indicate that (a) biological production in the northeastern AS is high compared to the northwestern BOB, (b) primary production at 21°N of the AS during the peak of the winter monsoon (December–January) is comparable to the production of the upwelling regions of the central and southeastern AS during the summer monsoon; (c) winter cooling along with low salinity cause large-scale thermal inversion (> 2.5°C) in the BOB and (d) in the northernmost part of the BOB, upper low-saline water restricts atmospheric cooling to the surface layer and inhibits convection.

THE northern Indian Ocean (IO), together with its two major basins, the Arabian Sea (AS) and the Bay of Bengal (BOB), is land-locked in the north by the Asian continent which separates the northern IO from the deep-reaching vertical convection areas of the Arctic Seas and the cold climatic regions of the northern hemisphere. BOB, the northeastern part of the IO, is completely separated from the northwestern part, the AS by the Indian peninsula. The northern IO is influenced by the seasonally reversing monsoonal wind^{1,2}. From June to September (summer monsoon), the winds² are predominantly from the southwest and velocities often exceed 14 m s⁻¹. From November to February, the winds reverse and are predominantly from the northeast with speed of ~5 m s⁻¹ (winter monsoon). Even though the two basins (AS and BOB) are located along the same latitudes and are influenced by the same seasons, they show marked differences. Over the AS, evaporation exceeds precipitation and high-saline waters (Arabian Sea High Saline Waters (ASHSW), Persian Gulf Waters (PGW) and Red Sea Water masses (RSW)) occupy the upper 1000 m. In contrast, over the BOB the precipitation through rainfall and river run-off exceeds evaporation, sustaining an upper layer of low-saline waters. Stratification in the surface layer of the bay is dominated by the salinity gradient rather than temperature gradient³.

During winter monsoon in the northern AS, cool and dry continental air brought by the prevailing northeast trade winds intensifies evaporation leading to surface cooling. This combined with reduced incoming solar radiation and high ambient surface salinity (> 36) drives convective mixing in the northern AS, resulting in upward transport of nutrients from the base of the thermocline⁴⁻⁶.

In recent years, the phenomenon of winter convection and associated enhanced primary production (PP) has been studied⁴⁻⁷ in the northern AS. However data on winter

production in the northeastern AS are scanty. In 1996, the Joint Global Ocean Flux Studies (JGOFS)–India group reported⁸ an increased PP (807 mgC m⁻² d⁻¹) compared to the previous intermonsoon period (310 mgC m⁻² d⁻¹) at 21°N, 67°E. This value is less compared to the winter production reported by the international JGOFS (1000–2000 mgC m⁻² d⁻¹) and the US-JGOFS (1452 mgC m⁻² d⁻¹) at comparable latitudes of the northwestern AS^{6,9}. JGOFS-India sampling was done during 3 February–4 March 1994 (lean winter monsoon period) and the International and US-JGOFS were from 11 January to 6 February 1995 and 30 November to 29 December 1995 (peak winter monsoon periods) respectively. The dataset that we present here is generated during the peak of the winter monsoon period (29 November–5 January 2000) from the northeastern AS and the station locations were more close to the JGOFS-India stations.

The hinterland of the northern and northwestern part of the BOB has tributaries and distributaries of five major rivers, the Ganges, Brahmaputra, Mahanadi, Godavari and Damodar, which considerably dilute the salinity of the BOB throughout the year. Rains over the BOB show strong seasonality. The southeastern coast of India has a winter rainfall maximum and the rest of the region has a summer monsoon maximum¹⁰. During winter monsoon, the surface salinity at 20°N is higher (27) compared to the summer monsoon (22)¹¹. Hydrographic data collected during the summer monsoon of 1989 along the east coast of India showed a narrow upwelling band of 40 km width along most of the coastline³. Since the region is one of the least explored areas of the IO, authentic and systematic seasonal studies on productivity patterns are fewer. The literature available for PP is mostly for the summer monsoon season, where observations do not agree. Studies up to 1976 reported low PP^{12,13} (120–310 mgC m⁻² d⁻¹, April/May 1951; 130–820 mgC m⁻² d⁻¹, April/May 1963; 160–240 mgC m⁻² d⁻¹, March/April 1975, 220–320 mgC m⁻² d⁻¹, August/September 1976). The possible reason suggested for the lower PP in the BOB was heavier cloud coverage and turbidity arising from sediment fluxes, which limit effective solar radiation in the upper euphotic column^{12,13}. More recent studies showed very high PP^{14,15} (140–5590 mgC m⁻² d⁻¹, 180–3410 mgC m⁻² d⁻¹), higher than the production in the AS during this period. The most recent study (2001)¹⁶ during the summer monsoon in the BOB by the JGOFS-India group observed PP values between 328 and 520 mgC m⁻² d⁻¹ and argues that, it is comparable with the PP of the AS during inter monsoon spring (oligotrophic period). During winter, PP in the shelf regions of the northern BOB is reported to be higher than the inter monsoon spring and summer monsoon season¹⁷. Increased water-column transparency and river run-off are likely to be the reason for the increased production during winter.

Nevertheless, during winter, like the northern AS, the air temperature of the northwestern BOB decreases con-

siderably ($\sim 2.5^{\circ}\text{C}$ drop compared to the southern region)¹¹. However, winter convection due to atmospheric cooling, and the subsequent manifestation on biological productivity in AS and BOB have not been studied earlier, on a comparative basis. The objectives of the present study are to (a) understand the magnitude of physical forcing in the AS and BOB during winter monsoon and its consequences on the physical characteristics of the upper water column; (b) understand the vertical distribution of chemical parameters (oxygen, nitrate, phosphate and silicate) and (c) generate a new dataset for biological parameters (phytoplankton standing stock, primary productivity, microzooplankton and mesozooplankton biomass) for both AS and BOB during winter monsoon, from which a comparison between both the basins could be attempted.

As part of Marine Research – Living Resources (MR–LR) Assessment programme of the Department of Ocean Development (DOD), New Delhi measurements were carried out during the winter monsoon period along the northwest and northeast coasts of India in two cruises of FORV *Sagar Sampada*. Cruise 190 (29 November–5 January 2001) was conducted in the northeast AS and cruise 198 (20 November–18 December 2002) was in the northwest BOB. The parameters measured include hydrography, PP, chlorophyll *a* (Chl *a*), mesozooplankton biomass (MZB) and microzooplankton biomass (MZPB). This communication is based on the samplings made at 13 hydrographic stations along three transects at 17, 19 and 21°N in the AS and 17, 19 and 20.5°N in the BOB (Figure 1). The biological productivity studies were made in two stations in each transect (A1–A6 in AS and B1–B6 in the BOB), grouped coastal (stations close to the coast) and oceanic (stations farthest from the coast).

The same methodology was followed in the AS and BOB. Surface meteorological parameters were collected

from all stations and a ship-based automated data acquisition software system was used to collect the meteorological parameters with an interval of 10 min throughout the ship track. The sea surface temperature (SST) was measured using a bucket thermometer, by keeping it in the water close to the surface. The mixed layer depth (MLD) is defined as the depth of the isoproperty surface layer, obtained by plotting profiles of temperature, salinity and density against depth. Water samples were collected for Chl *a*, PP and MZPB from 7 standard depths, viz. 0, 10, 20, 50, 75, 100 and 120 m (dissolved oxygen and nutrients samples were collected up to 200 m) using Niskin samplers. Sea-Bird electronic CTD was used to obtain the temperature and salinity profiles. CTD salinities were corrected against the values obtained by the Autosol (model 8400A, Guildline). The analyses of nitrate, phosphate and silicate were done using a Skalar San Plus autoanalyser and estimation of dissolved oxygen was carried out by the Winkler's method. Two litres of water from each standard depth was filtered through GF/F filters (nominal pore size 0.7 μm) to estimate Chl *a* spectrophotometrically (Perkin–Elmer UV/Vis) using 10 ml 90% acetone for extraction¹⁸ and PP was measured using ¹⁴C-technique¹⁹. Water samples were collected into four 300 ml polycarbonate bottles (Nalgene; Germany, three light and one dark), each from all the seven standard depths mentioned above for PP. Incubation was for 12 h (sunrise to sunset). Prior to incubation of ¹⁴C-series, 1 ml of $\text{NaH}^{14}\text{CO}_3$ (Board of Radiation and Isotope Technology, Mumbai) was added to each sample (5 μCi per 300 ml sea water). Mooring system was deployed for facilitating *in situ* incubation of PP samples. After the 12 h incubation, the samples were filtered through 47 mm GF/F filters under gentle suction. Then the filter papers were exposed to concentrated HCl fumes to remove excess inorganic carbon and kept in scintillation vials for subsequent estimation of ¹⁴C uptake. Next 5 ml of liquid scintillation cocktail (Sisco Research Laboratory, Mumbai) was added to the vials a day before analysis, and the activity counted in a scintillation counter (Wallac 1409 DSA, Perkin–Elmer, USA). The disintegration per minute (DPM) values were converted into daily production rates ($\text{mgC m}^{-2} \text{d}^{-1}$) using the appropriate formula¹⁹. Column Chl *a* (mg m^{-2}) and PP ($\text{mgC m}^{-2} \text{d}^{-1}$) were calculated by integrating depth values up to 120 m.

Mesozooplankton was collected with a multiple plankton closing net (Hydrobios, mouth area 0.25 m², mesh width 200 μm). Samples were collected from the base of the thermocline to the surface and all the collections were carried out during the day (mostly around the noon) to avoid the possible impact on biomass due to zooplankton vertical migration. Collection of microzooplankton was carried out by filtering 5 l of water samples from each depth, prefiltered gently through a 200 μm bolting silk to avoid the mesozooplankton and collected into black polythene bottles. Subsequently, samples were concentrated

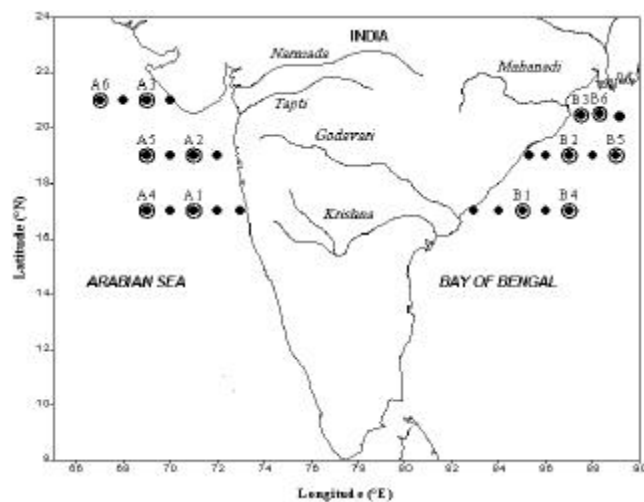


Figure 1. Station locations in the AS and BOB. Closed circles represent the hydrographic stations and closed circles surrounded by open circles denote positions where biological samplings were made.

by siphoning through a PVC tubing with its cod end fitted with a 20 µm Nitex screen for retaining all the microzooplankton of ≥ 20 µm size at the bottom of the carboy. Thus microzooplankton samples were concentrated to 100 ml volume and then preserved in 1–3% acid Lugol's solution. Samples were left to settle for more than 48 h in a settling chamber. Microzooplankton were analysed with an Olympus inverted microscope at 100–400 × magnification. The dimensions of ciliates and dinoflagellates were measured using a calibrated ocular micrometer. Biovolumes of organisms were determined using appropriate geometrical formulae and carbon content (pgC) was calculated using conversion ratio²⁰. Integrated MZPB with depth made up the standing stock per unit area.

Along the northeastern AS, surface winds were predominantly northeasterly with an average speed of ~ 6 m s⁻¹. Air-temperature distribution showed a diurnal oscillation and varied from 24 to 30°C and decreased northwards (Figure 2). The SST pattern also showed a decreasing

trend towards north and varied from 26 to 27.8°C, with an average of 27.2, 27 and 26.4°C respectively along the transects 17, 19 and 21°N. The sea surface salinity (SSS) showed weak lateral variation (35.2 to 36.8), which increased towards north. Generally, the MLD was deeper (average 60 m) towards the north, except at a few stations. Shallow MLD (~ 30 m) was observed at the station near the coast along 19°N. This could be due to the low winds (< 4 m s⁻¹) that prevailed over the respective locations.

In the northwestern BOB, wind pattern, surface pressure, air temperature and SST pattern were similar to that over the AS, but varied in magnitude. The surface winds were predominantly northeasterly, with an average speed of 5 m s⁻¹. Air temperature showed diurnal variability and

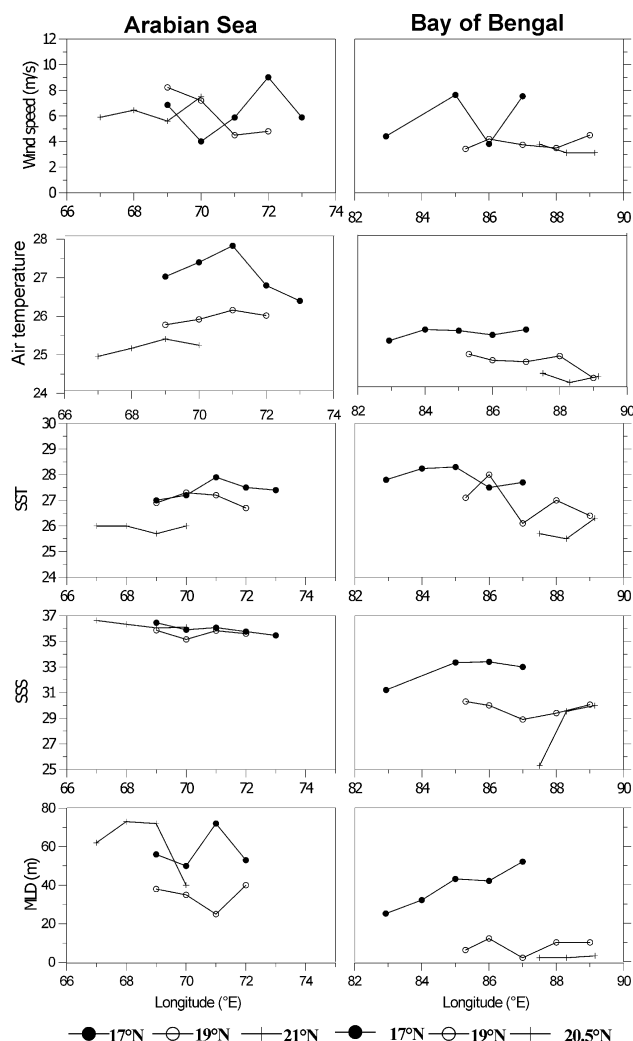


Figure 2. Distribution of wind speed, air temperature, sea surface temperature, sea surface salinity and mixed layer depth along the three transects in the AS and BOB.

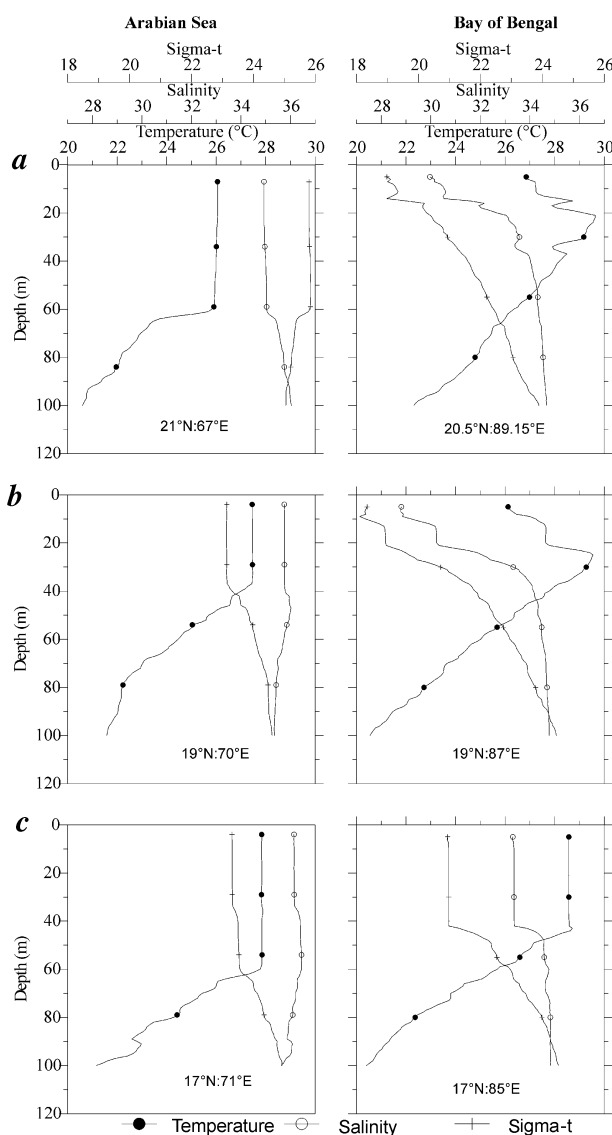


Figure 3. Vertical distribution of temperature, salinity and density at stations in the transects (a) 17°N, (b) 19°N and (c) 21°N in AS, 20.5°N in BOB in the northeastern AS and northwestern BOB.

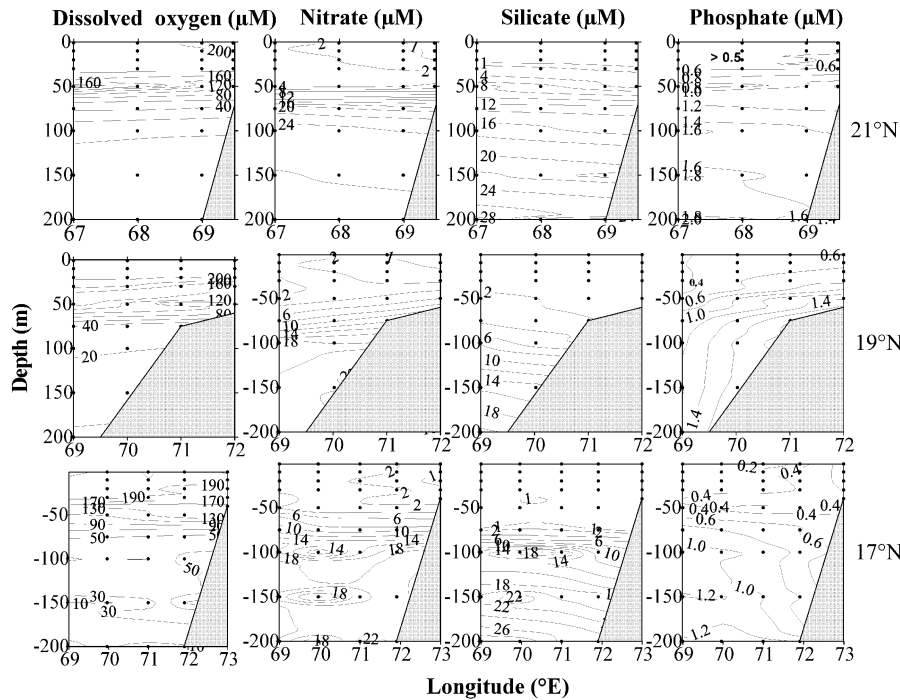


Figure 4. Vertical distribution of dissolved oxygen, nitrate, silicate and phosphate along transects 17°N (bottom), 19°N (middle) and 21°N (top) in the northeastern AS during winter monsoon.

ranged from 25 to 29°C and decreased northwards. The SST varied from 25.3 to 28.3°C and the pattern almost resembled that in the AS. Slightly higher temperature was observed along 17 and 20.5°N in the BOB compared to the respective transects along the AS. The low-saline waters in the northern BOB resulted a shallow mixed layer in this region (< 5 m). The MLD was shallower towards the coast and the deepest mixed layer was observed at the farthest station along 17°N, where relatively high salinity was observed; this indicated the least effect of river discharge. A special feature of the vertical structure was the thermal inversion in surface layers (Figure 3) that occurred immediately below the mixed layer. The amplitude of inversion increased towards north and reached > 2.5°C in the northernmost transect (Figure 3). In the northwestern BOB, low salinity has a strong influence on the density in the upper layers (Figure 3).

Large variation (2–5) in salinity with depth was a general feature in the BOB during the season. In the upper 100 m water column, salinity varied markedly with depth. Along 19 and 20.5°N the salinity gradients in the upper 100 m water column were 4–5, while stations at comparable latitudes of AS showed gradients of 0.3–1.5 (Figure 3).

The distribution of nitrate and silicate showed contrasting behaviour (Figures 4 and 5) in AS and BOB, although the atmospheric cooling prevailed at both sides. Presence of rich nitrate (> 2 µM) in the surface waters was the characteristic in the northernmost section of AS, but silicate and phosphate were relatively lower. Convective mixing in the northern AS is strong enough to erode the upper

portion of the thermocline and introduce more nitrate, but the higher concentrations of silicate and phosphate lie at much greater depths (Figure 4). Oxygen concentration in the upper 30 m was approximately 200 µM in AS and did not show any latitudinal variation.

Response in BOB to winter cooling, as evident from Figure 5, was quite different. The BOB showed depleted (almost undetectable) levels of nitrate and phosphate in the upper water column. Due to strong stratification, nitrate and phosphate remained at greater depths (0.5 µM at ~40 m and 0.4 µM at 30 m respectively). Enrichment of surface waters with silicate (2 µM at 20 m) at the northernmost transect (20.5°N) is obviously due to the influx of river discharge in that region. Oxygen distributions in the upper layers of the BOB were only slightly different from the AS with high concentrations along the northernmost transect (20.5°N).

At the coastal stations of the AS, integrated Chl *a* concentration ranged between 19 and 82 mg m⁻² (avg. 48.6 mg m⁻²) and PP varied from 373 to 1854 mgC m⁻² d⁻¹ (avg. 1081 mgC m⁻² d⁻¹). At the oceanic stations, the integrated Chl *a* ranged between 25 and 58 mg m⁻² (avg. 46.3 mg m⁻²) and PP varied from 731 to 1363 mgC m⁻² d⁻¹ (avg. 1147 mgC m⁻² d⁻¹). Maximum integrated Chl *a* concentration (82 mg m⁻²) and PP (1854 mgC m⁻² d⁻¹) were found at the coastal station at 21°N (Station A3). Moreover, latitudinal comparison showed that highest average Chl *a* and PP were at 21°N (avg. Chl *a* 69 mg m⁻², avg. PP 1608 mgC m⁻² d⁻¹), followed by 17°N (avg. Chl *a* 51.5 mg m⁻², avg. PP 1182 mgC m⁻² d⁻¹) and 19°N (avg.

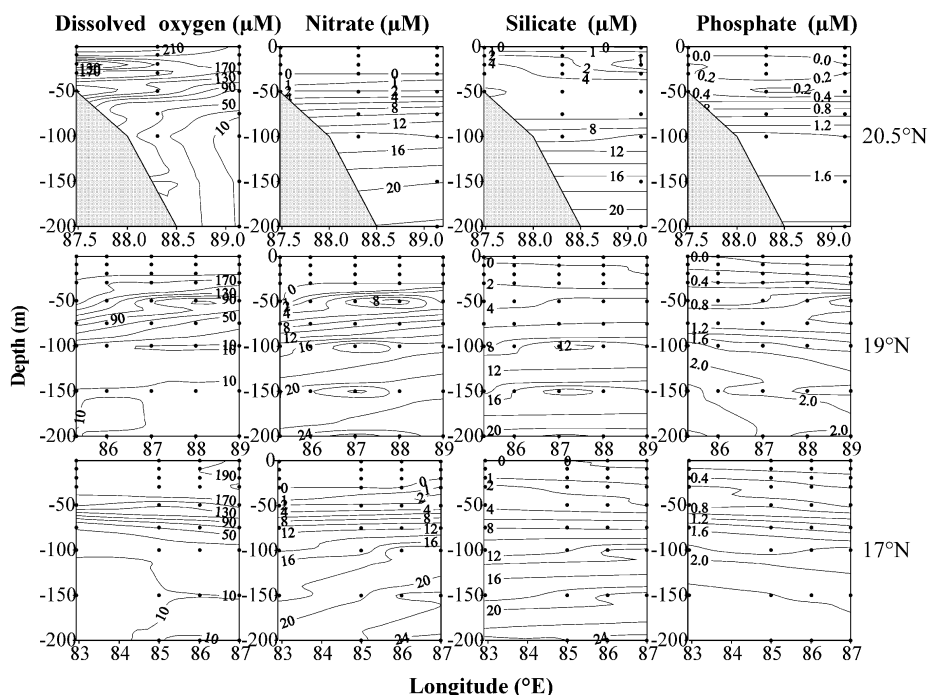


Figure 5. Vertical distribution of dissolved oxygen, nitrate, silicate and phosphate along transects 17°N (bottom), 19°N (middle) and 20.5°N (top) in the northwestern BOB during winter monsoon.

Chl *a* 22 mg m⁻², avg. PP 551 mgC m⁻² d⁻¹). Overall, during the study the AS had high Chl *a* concentration (avg. 47.5 mg m⁻²) and PP (avg. 1114 mgC m⁻² d⁻¹).

At the coastal stations of the BOB, integrated Chl *a* concentration ranged between 9 and 15 mg m⁻² (avg. 13 mg m⁻²) and PP varied from 115 to 187 mgC m⁻² d⁻¹ (avg. 149 mgC m⁻² d⁻¹). In the oceanic regions, Chl *a* concentration varied from 9 to 13 mg m⁻² (avg. 13 mg m⁻²) and PP from 87 to 164 mgC m⁻² d⁻¹ (avg. 133 mgC m⁻² d⁻¹) respectively. The maximum integrated Chl *a* (15 mg m⁻²) and PP (187 mgC m⁻² d⁻¹) were found at the coastal stations at 19°N (Station B2). Latitudinal comparison showed that higher average Chl *a* and PP were found along 19°N (avg. Chl *a* 14 mg m⁻², avg. PP 175 mgC m⁻² d⁻¹) followed by 17°N (avg. Chl *a* 11.5 mg m⁻², avg. PP 123 mgC m⁻² d⁻¹) and 20.5°N (avg. Chl *a* 9 mg m⁻², avg. PP 101 mgC m⁻² d⁻¹). Comparison between the AS and BOB showed that the AS held fivefold more Chl *a* (Figure 6 *a*) and tenfold more PP (Figure 6 *b*).

General pattern of the surface chlorophyll *a* distribution derived from satellite (Sea WiFS; Figure 7) further supports the actual measurements done on-board. Chlorophyll *a* distribution from Sea WiFS clearly showed higher concentration in the AS compared to BOB and in both the basins, coastal regions had maximum concentration.

The coastal regions of AS showed an average MZB of 175 mmolC m⁻². The biomass of the stations ranged between 137 and 198 mmolC m⁻². In the oceanic stations, average biomass was 168 mmolC m⁻². In the entire northern

AS, average biomass was 172 mmolC m⁻². Latitudinal comparison showed that 17°N and 19°N latitudes had higher MZB (190 and 179 mmolC m⁻² respectively) followed by 21°N (153 mmolC m⁻²). In the BOB, MZB biomass in the coastal and oceanic stations ranged between 30 and 60 mmolC m⁻² and 50 and 133 mmolC m⁻² respectively. The average MZB for northwestern BOB was 71 mmolC m⁻². Latitudinal comparison showed that 17°N had maximum MZB (92 mmolC m⁻²) followed by 19°N (81 mmolC m⁻²) and 20.5°N (40 mmolC m⁻²). Comparison between average MZB of AS and BOB showed that the former hold biomass more than twice the latter (Figure 6 *c*).

The coastal regions of the AS had a higher average MZPB (avg. 28.9 mmolC m⁻²) compared to the oceanic regions (avg. 23.2 mmolC m⁻²). Maximum average biomass observed was at 21°N (31.9 mmolC m⁻²) followed by 17°N (29.8 mmolC m⁻²) and least at 19°N (16.5 mmolC m⁻²). Maximum biomass (41.3 mmolC m⁻²) was obtained at the oceanic station of 21°N (Station A6) and the average biomass in the entire region was 26 mmolC m⁻². Coastal and oceanic regions of BOB had an average biomass of 12 mmolC m⁻² and 9 mmolC m⁻² respectively. Maximum average biomass was obtained at 17°N (29.8 mmolC m⁻²) followed by 19°N (11 mmolC m⁻²) and the least at 20.5°N. Average biomass of the region was 10.6 mmolC m⁻², which indicated that the BOB had lesser microzooplankton standing stock compared to AS (26 mmolC m⁻²; Figure 6 *d*).

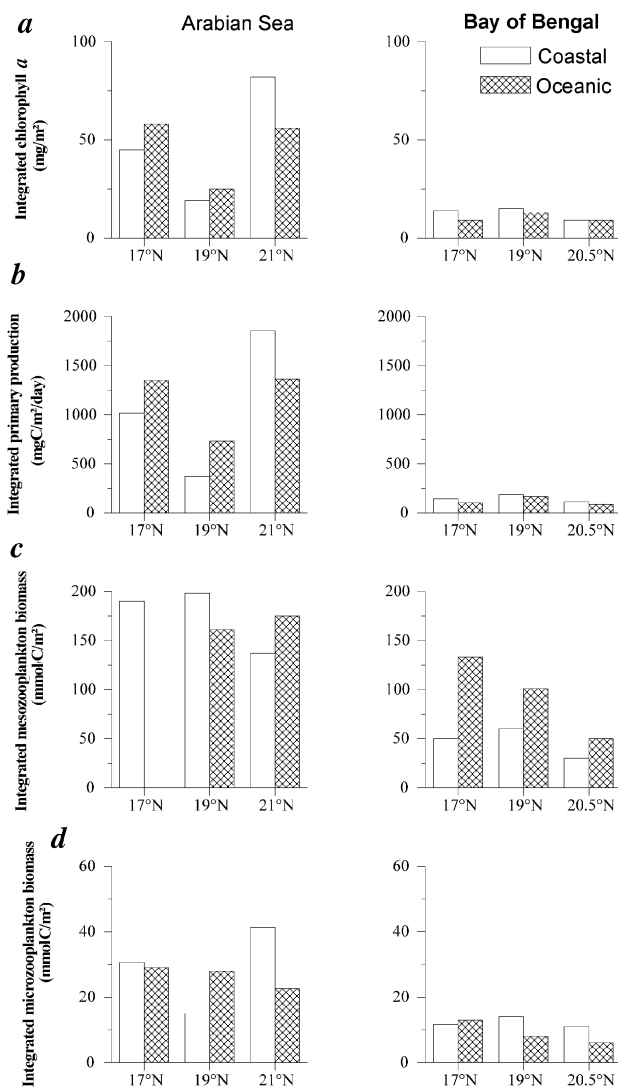


Figure 6. Distribution of integrated (a) chlorophyll *a*, (b) primary production, (c) mesozooplankton biomass and (d) microzooplankton biomass in the AS and BOB during winter monsoon.

The ASHSW, the PGW and the RSW make the AS highly saline. Consequently, heat loss by the winter cooling process triggers convective mixing. The deepening of mixed layer from southern to northern latitudes coincided with the intensification of winter, except at the coastal station along 19°N where shallow MLD (~30 m) was observed, and this could be due to the low winds (~4 ms⁻¹) that prevailed in the region. Comparatively low MLD was also observed at 17°N; 70°E where wind speed was low (<4 ms⁻¹). These observations indicate that even during winter MLD is not solely determined by atmospheric cooling alone, but by the combined effect of atmospheric cooling and wind speed.

The atmospheric conditions in the BOB were more favourable to the winter cooling processes. Relatively colder, dry air (humidity <60%) blew over the BOB than the northeastern AS (humidity >65%). The climatological

atlas of evaporation and latent heat flux²² corroborate the heat loss of the sea surface to the atmosphere by the winter cooling. In addition, the freshwater influx due to precipitation and run-off freshens the surface layers in the northern BOB. As a result, the cold freshwater in the surface layers stays stagnated, below which the temperature increases with depth resulting in thermal inversion. The low-saline waters compensate the static stability loss by thermal inversion. Many researchers have reported earlier on the BOB inversions^{18,23–25}. Thermal inversion mostly dominates during winter, which suggests that it is due to the freshwater influx and evaporative cooling over the region.

Using the climatological dataset, river discharge¹⁸ was computed for summer monsoon and winter monsoon. Strickland and Parsons found that the northwestern bay receives a discharge of 531×10^9 m³ and 59×10^9 m³ during summer and winter monsoons respectively. However, earlier studies in the BOB reported small-amplitude thermal inversion during summer even if being influenced by maximum river discharge^{3,18,23,25}. From our observations, it becomes obvious that winter cooling process is the major causative force for the large-scale inversion (amplitude >2°C) in the northern BOB along with the salinity gradient in the surface. During winter, due to atmospheric cooling, the surface layers attain low temperature but fail to impart it to the deeper waters owing to the lack of sinking and convective mixing. Maximum MLD obtained at the open ocean station at 17°N was due to the absence of freshwater influx, since this station was the farthest one from the hinterland. Large variations in salinity with depth (gradients of 2–5 in the upper 100 m water column) in the BOB are clear evidence of the enormous quantity of freshwater that northern BOB receives from the Mahanadi–Ganges–Brahmaputra river systems. On the contrary, the surface layers of the AS were highly saline due to the ASHSW, PGW and RSW, and the upper 100 m water column shows salinity gradients of 0.3–1.5 only.

Vertical distribution of nutrients in the AS and BOB was characterized by marked variations. In the AS, the upper 50 m water column possessed 2 μM nitrate which was a clear indication of convective mixing mechanism operating in the region. Interestingly, in the BOB the upper 50 m water was devoid of nitrate, which points out the low efficiencies of vertical mixing mechanisms operating in that region. The absence of nitrate in the upper water column of the BOB during winter monsoon has been reported earlier²⁶. High concentration of silicate (2 μM) and oxygen (>200 μM) in the surface layers of the northernmost stations could be a sign of river inputs. High Chl *a* (avg. 47.5 mg m⁻²) in the AS is attributed to high nutrient concentration by convective mixing. Higher chlorophyll concentration in the AS during the present study is further supported by the chlorophyll distribution derived from Sea WiFS. Highest average PP (1854 mg C m⁻² d⁻¹) obtained at the coastal station of the northernmost latitude coincided with the highest MLD

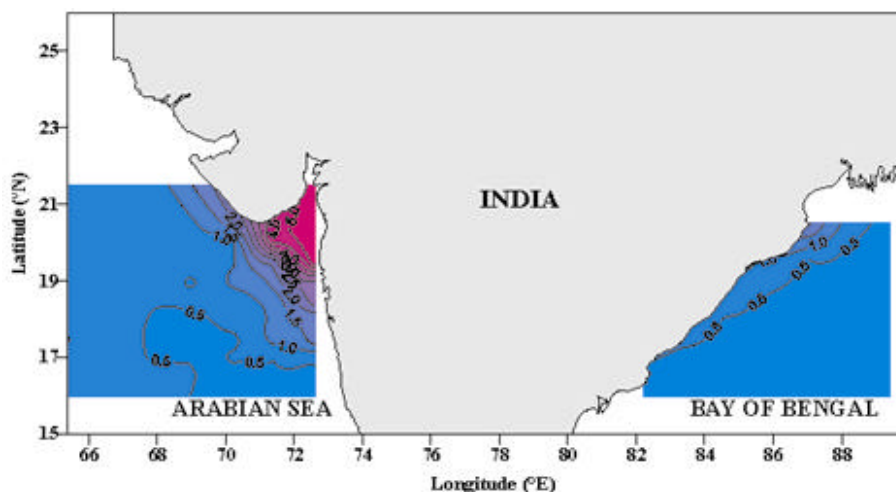


Figure 7. SeaWiFS chlorophyll *a* (monthly average) distribution for the AS and BOB during the respective periods.

(~80 m). Relatively low integrated Chl *a* and PP (avg. Chl *a* 22 mg m⁻², avg. PP 551 mgC m⁻² d⁻¹) observed along 19°N in the AS correspond with the low MLD in that transect.

But in the BOB, PP and Chl *a* were very low (avg. 117 mg m⁻² d⁻¹, avg. 10.3 mg m⁻² respectively) and low PP was due to the absence of nitrate and phosphate in the water column. In the AS, the northernmost latitude (21°N) sustained high phytoplankton biomass and production (avg. Chl *a*. 69 mg m⁻², avg. PP 1608 mgC m⁻² d⁻¹), but in the BOB the northernmost latitude had the least values (avg. PP 69 mgC m⁻² d⁻¹, avg. Chl *a* 9 mg m⁻²). Higher PP in the northernmost latitude of the AS could be due to the intensification of winter towards north, which increased the mixed layer, but the northernmost latitudes of the BOB receive maximum influence from freshwater, which leads to strong stratification of the upper waters.

For the AS, comparison between the average integrated Chl *a* and PP obtained during the present study (Chl *a* 47.5 mg m⁻² and PP 1114 mgC m⁻² d⁻¹) with Indian JGOFS (Chl *a* 34.4 mg m⁻² and PP 870 mgC m⁻² d⁻¹) showed that the former average is much higher than the latter. During the present investigation the sampling was carried out during the peak of winter (29 November–5 January 2000), while the Indian JGOFS studies were during the late winter monsoon (3 February–4 March 1994). This could possibly be the reason for the higher PP and Chl *a* in the present study. Interestingly, our observations were quite comparable with the international JGOFS (1000–2000 mgC m⁻² d⁻¹)⁶ in the northwestern AS, even though their study area was in the central and northwestern AS. Moreover, the present study revealed that the cooling during winter is more or less equal in the northern parts of the BOB and AS.

MZB in the AS (172 mmolC m⁻²) was higher than that in the BOB (71 mmolC m⁻²). Although the primary source of nutrition for mesozooplankton is through the phyto-

plankton, the difference between the two areas (AS and BOB) was not as drastic as for phytoplankton biomass (the latter about fivefold against more than one and a half for the former). Obviously, a one-to-one relationship between primary and secondary producers does not exist. Other pathways for nourishment of secondary producers could be derived through the microbial loop or even from particulate organic matter⁷.

Low MZPB (10.6 mmol m⁻²) in the BOB was attributed to the very low PP and mesozooplankton standing stock, which in turn forms the potential source of dissolved organic carbon (DOC) on which bacteria and heterotrophic flagellates start building up. Unfortunately, we do not have measurements for DOC, heterotrophic flagellates and bacterial counts, which are thought to be essential for the elucidation of the microbial food-web relations.

Our studies revealed that during winter both northeastern AS and northwestern BOB experience more or less equal atmospheric cooling, but the consequences of this process produce converse results along the two regimes. In the AS, the winter cooling processes lead to densification of surface water, which results in convective mixing and deepening of the mixed layer. Injection of nutrients to the surface layers by convective mixing promotes high biological production. During the study, winter cooling generated PP values as high as 1854 mgC m⁻² d⁻¹ at the northernmost latitude. This is higher than the reported production (1760 mgC m⁻² d⁻¹) of the southeast AS during the southwest monsoon (upwelling period) and suggests that winter production in the northern AS is roughly of the same magnitude as the upwelling production of the south. While along the northwestern BOB, winter cooling process results in strong thermal inversion and shallow mixed layer. The upper freshwater layer behaves like a cap and restricts the impact of atmospheric cooling to the thin surface layers, avoiding the chances of sinking by densification. Undetectable amounts of nitrate in the top

50 m waters of the BOB are an indication of the oligotrophic nature of the water that eventually leads to very low biological production.

1. Banse, K., *Deep-Sea Res.*, 1987, **34**, 713–723.
2. Bauer, S., Hitchcock, G. L. and Olson, D. B., *Deep-Sea Res.*, 1991, **38**, 531–533.
3. Shetye, S. R., Shenoi, S. S. C., Gouveia, A. D., Michael, G. S., Sundar, D. and Nampoothiri, G., *Continent. Shelf Res.*, 1991, **11**, 1397–1408.
4. Prasanna Kumar, S. and Prasad, T. G., *Curr. Sci.*, 1996, **71**, 834–841.
5. Prasanna Kumar, S. *et al.*, *Deep-Sea Res. II*, 2001, 1115–1126.
6. Barber, R. T. *et al.*, *Deep-Sea Res. II*, 2001, **48**, 1127–1172.
7. Madhupratap, M., Prasanna Kumar, S., Bhattathiri, P. M. A., Dileep Kumar, M., Reghu Kumar, S., Nair, K. K. C. and Ramaiah, N., *Nature*, 1996, **384**, 549–552.
8. Bhattathiri, P. M. A., Aditi Pant, Surekha Sawant, Gauns, M., Matondkar, S. G. P. and Mohanraju, R., *Curr. Sci.*, 1996, **71**, 857–862.
9. Veldhuis, M. J. W., Kraay, G. W., Van Bleijswijk, J. D. I. and Baars, M. A., *Deep-Sea Res. I*, 1997, **44**, 425–449.
10. Ramage, C. S., Climate of the Indian Ocean north of 35°S. In *World Survey of Climatology, Climates of the Oceans* (ed. Van Loon, H.), Elsevier, Amsterdam, 1984, vol. 15, pp. 603–659.
11. Varkey, M. J., Murthy, V. S. N. and Suryanarayana, A., Physical Oceanography of Bay of Bengal, In *Oceanography and Marine Biology: An Annual Review*, UCL Press, 1996, vol. 34, pp. 1–70.
12. Radhakrishna, K., *Indian J. Mar. Sci.*, 1978, **7**, 58–60.
13. Radhakrishna, K., *Indian J. Mar. Sci.*, 1978, **7**, 94–98.
14. Devassy, V. P., Bhattathiri, P. M. A. and Radhakrishna, K., *Maha-sagar*, 1983, **16**, 443–447.
15. Bhattathiri, P. M. A., Devassy, V. P. and Radhakrishna, K., *Maha-sagar*, 1980, **13**, 315–323.
16. Madhupratap, M. *et al.*, *Deep-Sea Res. II*, 2002, **50**, 881–896.
17. Gomes, H. R., Goes, J. I. and Saino, T., *Continent. Shelf Res.*, 2000, **20**, 293–311.
18. Strickland, J. D. H. and Parsons, T. R., In *A Practical Handbook of Sea Water Analysis*, Bull. Fish. Res. Board Can., 1972, 2nd edn, vol. 167, p. 310.
19. UNESCO, Protocols for the Joint Global Ocean Flux Study, Manual and Guides, 1994, vol. 29, p. 170.
20. Gifford, D. J. and Caron, D. A., ICES, *Zooplankton Methodology Manual*, Academic Press, New York, 2000.
21. Hastenrath, S. and Lamb, P. J., *Climatic Atlas of the Indian Ocean, Part. 1: Surface Climatic and Atmospheric Circulation*, The University of Wisconsin Press, Wisconsin, 1979, p. 104.
22. Shetye, S. R. *et al.*, *J. Geophys. Res.*, 1996, **101**, 14011–14025.
23. Han, W., McCreary, J. P. and Kohler, K. E., *J. Geophys. Res.*, 2001, **106**, 6895–6916.
24. Pankajakshan, T., Gopalakrishna, V. V., Muraleedharan, P. M., Reddy, G. V., Nilesh, A. and Shenoi, S., *Deep-Sea Res. I*, 2002, **49**, 1801–1818.
25. Rao, C. K., Naqvi, S. W. A., Kumar, M. D., Varaprasad, S. J. D., Jayakumar, D. A., George, M. D. and Singbal, S. Y. S., *Mar. Chem.*, 1994, **47**, 279–290.

ACKNOWLEDGEMENTS. This work was carried out under the Marine Research–Living Resources (MR–LR) Assessment programme with financial assistance from the DOD, New Delhi. We thank the Director, National Institute of Oceanography (NIO), Goa for the facilities provided. We also thank NASA, USA and Dr T. Suresh, NIO, Goa for the Sea WiFS chlorophyll data. R.J. and P.A.M. thank CSIR, New Delhi for financial support.

Received 12 November 2003; revised accepted 26 May 2004

Low period variability in Tropical Rainfall Measuring Mission Microwave Imager measured sea surface temperature over the Bay of Bengal during summer monsoon

Anant Parekh, Abhijit Sarkar*, Shivani Shah and M. S. Narayanan

Meteorology and Oceanography Group, Space Applications Centre, Ahmedabad 380 015, India

Sea surface temperature measured by the Tropical Rainfall Measuring Mission Microwave Imager (TMI) over the Bay of Bengal during monsoon was found to exhibit a low-period intra-seasonal mode of 8–16 days, in addition to the 30–60 days mode. This unique feature is attributed to the coherent response of the top freshwater layer, formed due to high precipitation and river run-off, to synoptic atmospheric monsoon processes. These results were obtained through Fourier, Morlet wavelet and time series analyses applied on TMI and buoy data of June–September during 1998–2001.

SEA surface temperature (SST) displays variability over a wide range of space- and time-scales. Over the tropical oceans, SST variability has been shown to be associated with the oscillations of a variety of weather patterns. The most pronounced oscillations in SST are known to occur over the Bay of Bengal (BoB) besides the equatorial western Pacific Ocean¹. The recent observations by space-borne microwave sensors of SST in the tropical oceans under the influence of cloudiness and precipitation, have further enriched the understanding of its variabilities.

Variability in meteorological and oceanographic parameters over the monsoon regions of north Indian Ocean, consisting of the Arabian Sea (AS) and the BoB, continues to be the focus of active research on monsoon variability². Yasunari³, and Sikka and Gadgil⁴ found two dominant periodicities of around 40 and 15 days in the fluctuations of cloudiness over the northern Indian Ocean (IO) during summer monsoon. Fluctuations of the 40 day period were shown to represent the marked northward movement of the cloudiness from the equatorial zone to the mid-latitudes, while the 15-day period mode seems to correspond with the movement of equatorial monsoonal disturbances. Murakami⁵, and Krishnamurti and Bhalme⁶ have also noted a period of around two weeks for the alteration between active and inactive phases of monsoon for near-normal rainfall years. In a recent study based on the spectral analysis of observations made during the Bay of Bengal Monsoon Experiment (BOBMEX), Hareeshkumar *et al.*⁷ found prominent peaks at around 10.6 days in the V-

*For correspondence. (e-mail: sarkar_abhi2000@yahoo.com)